



# The *in vitro* inhibition effect of 2 nm gold nanoparticles on non-enzymatic glycation of human serum albumin

Champika Seneviratne, Radha Narayanan, W. Liu, J.A. Dain \*

Department of Chemistry, University of Rhode Island, Kingston, RI 02881, USA

## ARTICLE INFO

### Article history:

Received 9 April 2012

Available online 10 May 2012

### Keywords:

Gold nano-particles

Human serum albumin

Glyceraldehydes

Glycation

High performance liquid chromatography

## ABSTRACT

The reaction of amino groups of protein and the carbonyl groups of reducing sugar molecules, non-enzymatically induce a series of chemical reactions that form a heterogeneous group of compounds known as advanced glycation end products (AGEs). The accumulation of AGEs is associated with various disease conditions that include complications in diabetes, Alzheimer's disease and aging.

The current study monitored the extent of non-enzymatic glycation of human serum albumin (HSA) in order to estimate the formation of HSA related AGEs in the presence of 2 nm gold nanoparticles. The rate of glycation was evaluated using several analytical methods. Physiological concentrations of HSA and glyceraldehyde mixtures, incubated with various concentrations of negatively charged 2 nm gold nanoparticles, resulted in a lower reaction rate than mixtures without 2GNP. Moreover, increasing concentrations of gold nanoparticles exhibited a pronounced reduction in AGE formation. High performance liquid chromatography, UV-visible spectroscopy and circular dichroism analytical methods provide reliable techniques for evaluating AGE formation of HSA adducts.

© 2012 Elsevier Inc. All rights reserved.

## 1. Introduction

Non-enzymatic glycation reaction plays an important role in human physiology. This reaction occurs as a result of the interaction of the carbonyl groups of sugars with the free amino groups of proteins to form Schiff base adducts [1]. Schiff bases undergo Amadori rearrangements and follow by a series of reactions that can include cyclization, oxidation, and dehydration to form more stable advanced glycation end products (AGEs) [2]. These adducts were observed to form *in vitro* as well as *in vivo* when they have been linked with long-term complications of progressive disease conditions in diabetes, Alzheimer's and atherosclerosis [3–5]. In addition, structural modification of proteins by sugars alters the percentage of alpha helical content of these proteins, consequently resulting in functional changes of proteins [6].

Earlier studies have demonstrated that free amino groups of human serum albumin (HSA), the most abundant protein in plasma, can non-enzymatically react with reactive carbonyl groups of D/L glyceraldehyde (GA) to form glycation adducts [7]. This present study investigates the effect of gold nanoparticles on the rate of HSA related AGE formation.

The emergence of new nanostructured materials could involve their use in disease prevention and diagnosis [8]. Metallic

nanoparticles are often used as non-enzymatic catalysts in the production of redox active biosensors [9]. Gold nanoparticles (GNPs), in particular, are among the most commonly used nanostructures in biological applications. For example, GNPs have been used for therapeutic applications in the treatment of chronic lymphocytic leukemia by increasing drug efficacy due to their biocompatibility, high surface area, and practical ability of surface functionalization [10,11]. GNPs can conjugate with different globular proteins like bovine serum albumin [12] and cytochrome c [10,13]. GNPs can be seeded on alpha crystalline protein at physiological pH. Glycation on GNP seeded protein is pH dependent [14]. Interestingly, GNP also has been used to determine the glycation status of proteins, where GNP modified alpha crystalline and human hemoglobin were found to be resistant to glycation by fructose [14]. Amino groups in proteins are speculated to be the seeding sites for GNP and this was found by analyzing GNP seeding on fructosylated hemoglobin molecules [15]. An analysis of CD and Fourier transform infrared techniques (FTIR) of GNP seeded hemoglobin has shown that seeded GNP induces a stable and fixed protein structure independent of the glycation status of the protein [16]. Inhibition of AGE formation has been reported with gold and silver nanoparticles [14,17].

The objective of this study was to investigate and evaluate the rate and extents of the AGE formation in the presence of varied concentrations of 2 nm GNP (2GNP) and to utilize a combination of reliable analytical methods to analyze the HSA related AGEs.

\* Corresponding author. Address: Department of Chemistry, 51, Lower College Road, Kingston, RI 02881, USA. Fax: +1 401 874 5072.

E-mail address: [jdain@chm.uri.edu](mailto:jdain@chm.uri.edu) (J.A. Dain).

## 2. Materials and methods

### 2.1. Chemicals and reagents

GA and low metal-ion-containing HSA were purchased from Sigma Chemical (St. Louis, MO, USA). Citrate reduced stable aqueous colloidal solution of  $1.5 \times 10^{14}$  particles/mL spherical 2GNP was purchased from Ted Pella Inc. (Redding, CA, USA). Disposable UV transparent cuvettes (12.5 × 12.5 × 36 mm) were obtained from Fisher Scientific (New Lawn, NJ, USA). Unless otherwise indicated, all other reagents and solvents were of analytical grade and were purchased from Sigma–Aldrich Chemical (St. Louis, MO, USA).

### 2.2. Experimental mixtures preparation

Stock solutions of 105 mg/mL HSA and 60 mM GA were prepared separately in 0.1 M phosphate buffered saline (PBS) of pH 7.2. Two experimental reaction mixtures were prepared as stated below and the formation AGEs was monitored over time.

- Thirty millimolar GA and 35 mg/mL HSA with and without 2GNP ( $5 \times 10^{13}$  or  $1.5 \times 10^{13}$  particles/mL) in a final volume of 2 mL of the PBS at pH 7.2.
- HSA was pre-incubated with  $5 \times 10^{13}$  or  $1.5 \times 10^{13}$  particles/mL of 2GNP for 7 days at 37 °C before adding 30 mM GA.

All reaction mixtures were then incubated for 12 days under sterile conditions at 37 °C. Samples of 10-day incubation were used to HPLC, CD and FTIR analysis.

Blanks, HSA (35 mg/mL) and GA (30 mM) alone, were also incubated for the same length of time. Aliquots were drawn from the incubated reaction mixtures at five-day intervals and were stored in –20 °C until analyzed. For the purpose of removing remaining traces of reducing agents in the matrix, 2GNP was ultra-centrifuged for 2.5 h at  $2 \times 10^4$  rpm and the original matrix was removed. Then the concentrated 2GNP is dissolved in deionized water before analysis. Concentrations of 2GNP solutions after centrifuging were determined by concentration vs. absorbance ( $\lambda = 225$  nm) calibration curves.

### 2.3. UV-visible spectroscopy

Absorbance spectra were obtained on a SpectroMax M<sub>2</sub> spectrophotometer (Molecular Devices, Sunnyvale, CA, USA) across the wavelength range 270–500 nm using UV-transparent plastic, 96 well plates. All samples were diluted 20-fold before analysis, and all aliquots of the incubated reaction mixtures were analyzed for UV absorbance at 279 nm. Based on repeated scanning from 250 to 700 nm, these wavelengths are found to be optimal for detecting AGE.

### 2.4. High performance liquid chromatography analysis

HPLC analysis was performed on a Hitachi analytical HPLC system comprising a L-7100 low-pressure gradient pumps, L-7200 sequential auto-sampler and a high sensitivity diode array detector (190–800 nm) and managed by D-7000 HPLC System Manager software. The products formed in the incubated mixtures of HSA and GA with different concentrations of 2GNP and were identified on a Phenomenex Jupiter 5 $\mu$ , 300 Å, C<sub>4</sub>, HPLC column (250 mm × 4.6 mm × 5  $\mu$ m). Mobile phases A and B were 0.1 M aqueous ammonium acetate and 100% HPLC analytical grade acetonitrile, respectively. A stepwise elution of 90:10 of B:A of the mobile phases was applied for 15 min followed by 10:90 of B:A of mobile phases for another 15 min in the entire analysis. Prior to HPLC analysis, all the

solvents were filtered with 0.45  $\mu$ m membranes (Millipore, Billerica, MA, USA) and degassed for 15 min before use. All the profiles were obtained at fixed wavelength of 279 nm. The accuracy and reproducibility of the HPLC method was confirmed to be within 5% based on repeated testing.

### 2.5. Circular dichroism analysis

CD spectra of HSA–GA mixtures treated with different concentrations of 2GNPs and control samples were recorded in the far-ultraviolet region (190–250 nm) on a Jasco J-720 spectropolarimeter (Tokyo, Japan) using a quartz cuvette of 1 mm path-length. Spectra obtained are averages of 10 consecutive scans performed using a bandwidth of 1 nm, response time of 2 s and a scan speed of 20 nm/min and baseline corrected by subtracting corresponding blanks.

### 2.6. Fourier transformation infrared spectroscopy

FTIR spectroscopy was used to investigate the changes in protein structure reacted with 2GNP and GA. Buffer subtracted transmission spectra were recorded in the wavenumber range of 600–4000 cm<sup>–1</sup> using a Perkin Elmer spectrum 100 FTIR spectrometer (PerkinElmer, Inc., Shelton, CT, USA).

## 3. Results

Analytical studies were performed with protein mixtures containing 2GNP estimating the difference of UV absorbance and secondary structure of HSA. With HSA–GA mixtures, 2GNP were found to produce substantial change in non-enzymatic reactivity. The result described henceforth is focused on the effect of 2GNP in HSA glycation by GA.

### 3.1. Formation of new AGE adduct

Fig. 1A shows UV absorbance (279 nm) profiles of incubation mixtures containing a constant concentration of HSA (35 mg/mL), GA (30 mM) and various concentrations of 2GNP at 37 °C for 12 days. Blanks were HSA and GA, alone which were incubated for similar lengths of time as the experimental samples.

Since the controls of GA or HSA alone did not show a significant change in absorbance reading, the increase of absorbance over time in case a in Fig. 1A is strictly due to products of non-enzymatic reaction and the variation of absorbance readings reflected the extent of products formed in the medium. Data presented in Fig. 1A cases b and c revealed that the increases in absorbance intensity were directly related to the concentration of 2GNP and incubation time. In case c, increasing the GNP concentration results in a significant reduction in the absorption spectra, which indicates that the presence of high concentrations of the GNP in the reaction mediums resulted in a reduction of the formation of new adducts. The absorbance measurements of HSA–GA mixtures with GNP ( $5 \times 10^{13}$  or  $1.5 \times 10^{13}$  particles/mL) were increased within first 3 days and eventually fell below that of the control mixtures of HSA–GA without GNP at 10 days incubation and mixtures contained  $5 \times 10^{13}$  particles/mL of 2GNP showed prominent reduction of UV absorbance readings than that of the mixtures with lower concentration of 2GNP. This finding confirms that GNP reduces the extent of new adduct formation after incubating for 10 days and also indicates that 2GNP at  $5 \times 10^{13}$  particles/mL concentration significantly inhibits non-enzymatic AGE formation of HSA.

Fig. 1B shows UV absorbance (279 nm) profiles of mixtures of GA added to the pre-incubated mixtures of HSA–2GNP solutions (c and d) and further incubated for 12 days. Fig. 1B-c and -d absorbance

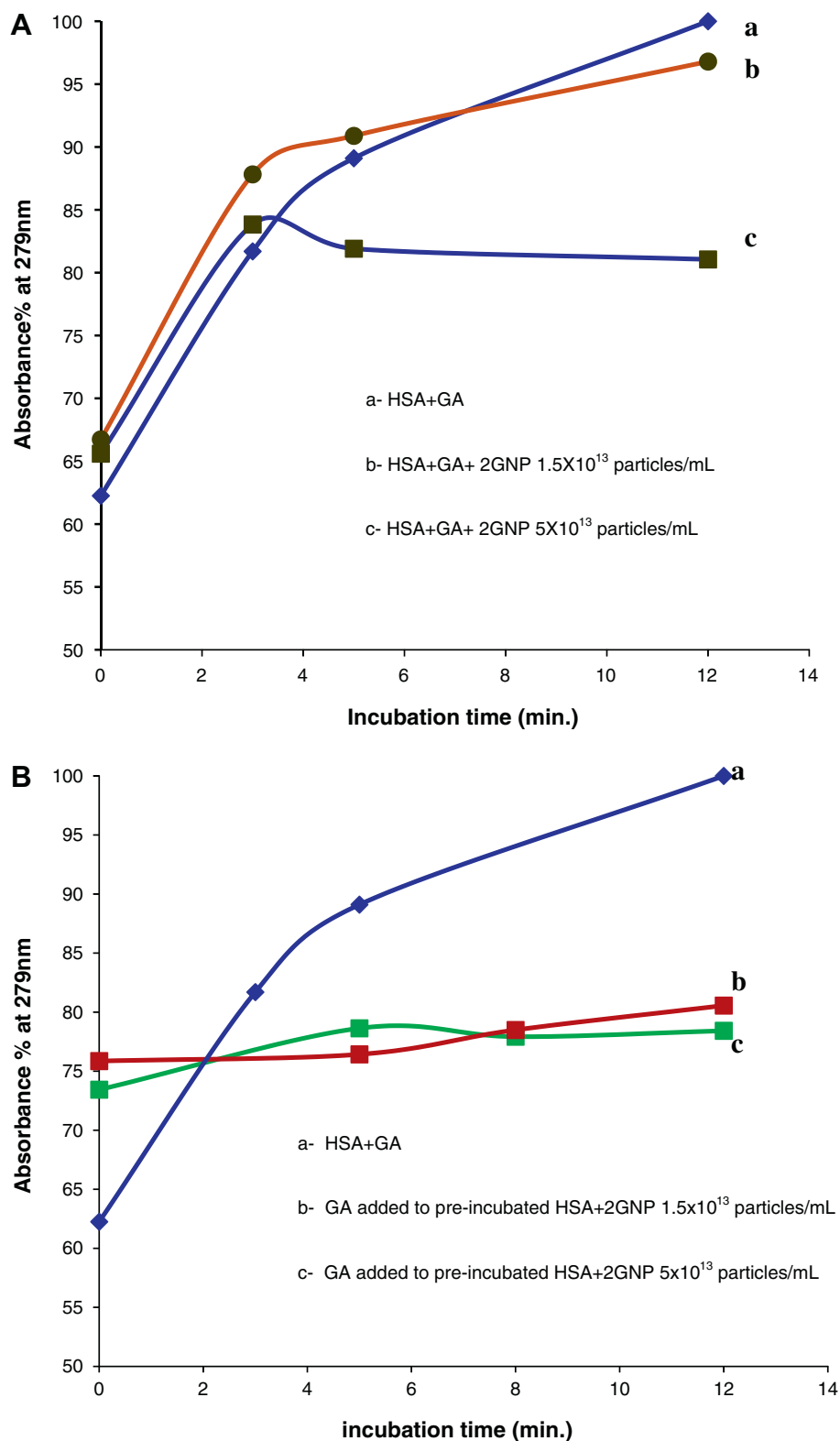


**Fig. 1.** UV absorbance spectral profiles of HSA and GA with and without 2GNP. (A) UV absorbance profiles of mixtures of HSA (35 mg/mL)–GA (30 mM) incubated with and without various concentrations of 2GNP at 37 °C for 12 days. (B) UV absorbance profiles of mixtures of GA (30 mM) added to pre-incubated HSA (35 mg/mL) with various concentrations of 2GNP and continued incubation for 12 days at 37 °C. UV absorbance readings were taken at 279 nm. All data points represent the averages of three replicate measurements.

profiles of HSA–2GNP–GA mixtures of both concentrations ( $5 \times 10^{13}$  or  $1.5 \times 10^{13}$  particles/mL) showed a dramatic reduction of absorbance readings compared to control HSA–GA solutions

incubated without 2GNP (a). This observation indicates that there is a notable reduction of the formation of new adducts when sugar reacts with pre-incubated HSA and gold nanoparticles. Moreover,

no significant difference was observed between c and d absorbance curves, indicated that the new AGE adduct formation is independent of the 2GNP concentration when HSA is pre-incubated with nanoparticles. This result is further confirmed by HPLC and CD profiles.

### 3.2. AGE formation in HSA–GA–2GNP mixtures

Fig. 2A shows the HPLC elution profiles of HSA (35 mg/mL) and GA (30 mM) with and without 2GNP which were incubated for 10 days at 37 °C. Under the same elution conditions, HSA alone (Fig. 2A-a) eluted at 13.7 min. and GA did not show a separate peak at 279 nm. A series of new peaks that emerged and increased in intensity over time represent formation of several AGE species. According to the intensities of those new peaks, peak numbered 2, 3, 4, 5, increased and the peak numbered 1, which represent unmodified HSA decreased simultaneously. This indicates HSA had been modified by GA to form new AGE products. HSA with GA elution profile (Fig. 2A-b) showed four additional peaks numbered 2, 3, 4, and 5, eluted at retention times 12.9, 8.7, 8.2, and 7.4 min respectively, whereas profiles of HSA–GA with 2GNP at  $1.5 \times 10^{13}$  particles/mL concentration (Fig. 2A-c) and HSA–GA with 2GNP ( $5 \times 10^{13}$  particles/mL) (Fig. 2A-d) indicated only three AGE species formed, a result confirms that fewer AGE species are formed in the presence of 2GNP. Furthermore, these HPLC profiles demonstrated that the formation of AGEs was dependent on 2GNP concentration, a conclusion reached after comparing the profiles of the incubated HSA–GA mixtures with various concentrations of 2GNP. Compared to profiles of b and c (Fig. 2A), the intensity of peak 2 was greatly diminished in the profile of HSA–GA with higher concentration ( $5 \times 10^{13}$  particles/mL) of 2GNP mixture (d), indicating decreased heterogeneity of AGEs at high 2GNP concentrations. This result coincided with observed lowering of UV absorbance data at 2GNP  $5 \times 10^{13}$  particles/mL concentrations than that of the mixtures with lower concentrates of 2GNP.

Fig. 2B shows the HPLC profiles of GA added to the pre-incubated HSA and 2GNP mixtures and further incubated for 10 days. Compared to the control HSA–GA mixture without GNP (Fig. 2B-a), profiles b and c both demonstrated prominent diminution of peak 4 and the similar intensities of peaks 2 and 5. This observation led to the conclusion that after conjugation with 2GNP, HSA showed special properties as it reacted with GA to form the same number of AGE species (Fig. 2B peak number 2, 3, and 5), each to the same concentration, and at the same rate. This observation is congruent with the finding of a recent report that bovine serum albumin coated with GNPs were more stable molecular aggregates and this stability is assumed to be imparted by steric and electrostatic interactions between nanoparticles and the protein [19].

The diminution of peak number 4 (Fig. 2B-b and -c) when GA reacts with pre-incubated HSA and 2GNP, and its presence in the HPLC profile of mixtures of HSA–GA without 2GNP, leads to the assumption that certain glycation sites are notably hindered by 2GNP preventing formation of specific AGE species represented by peak 4 in Fig. 2B-a.

### 3.3. HSA secondary structure change

Fig. 3 shows typical CD curves of HSA, HSA by GA, and glycated HSA by GA in the presence of 2GNP, in which each is incubated for 10 days. The CD curve of HSA showed a larger deviation indicating that HSA had the maximum of  $\alpha$ -helical content and conversely, HSA and GA mixture incubated for 10 days showed marked reduction of deviation representing diminution of  $\alpha$ -helical content is due to modification of HSA structure by GA.

Fig. 3A shows the amount of  $\alpha$ -helical content of HSA secondary structure when HSA was incubated with GA and different concentrations of 2GNP ( $1.5 \times 10^{13}$  or  $5 \times 10^{13}$  particles/mL). As compared

to CD measurements of HSA–GA control, more  $\alpha$ -helical content of the protein retained in mixtures with 2GNP indicating the extent of HSA modification in the presence of 2GNP was reduced. These profiles showed more  $\alpha$ -helix content remained in HSA secondary structure when the mixtures contained  $5 \times 10^{13}$  particles/mL concentration of 2GNP than that of the mixtures with  $1.5 \times 10^{13}$  particles/mL of 2GNP, indicating the reduction of structural modification of HSA is dependent on concentration of 2GNP.

In addition, when GA was added to previously incubated HSA–2GNP mixtures, both concentrations of GNP demonstrated relatively small change in HSA secondary structure (Fig. 3B). These two CD curves of HSA–2GNP–GA mixtures showed insignificant difference in deviation from each other and this shows their  $\alpha$ -helices contents are fairly similar. This observation demonstrates that GA reacts with pre-incubated HSA–2GNP, in a concentration independent manner. Consistent with prior reports, this study also assumes 2GNP of both concentrations may have altered the secondary structure of HSA in a similar manner leading to identical conformational structure [16]. Evidently, the interaction with 2GNP prior to reacting with GA, HSA demonstrates significant retention of structural characteristics as compared to the HSA–GA incubated without 2GNP. Although HPLC results showed reduction of certain AGE product formation in the presence on 2GNP, CD result confirms a similar effect of 2GNP on altering secondary structure of HSA. FTIR results of the current study also produced a consistent result.

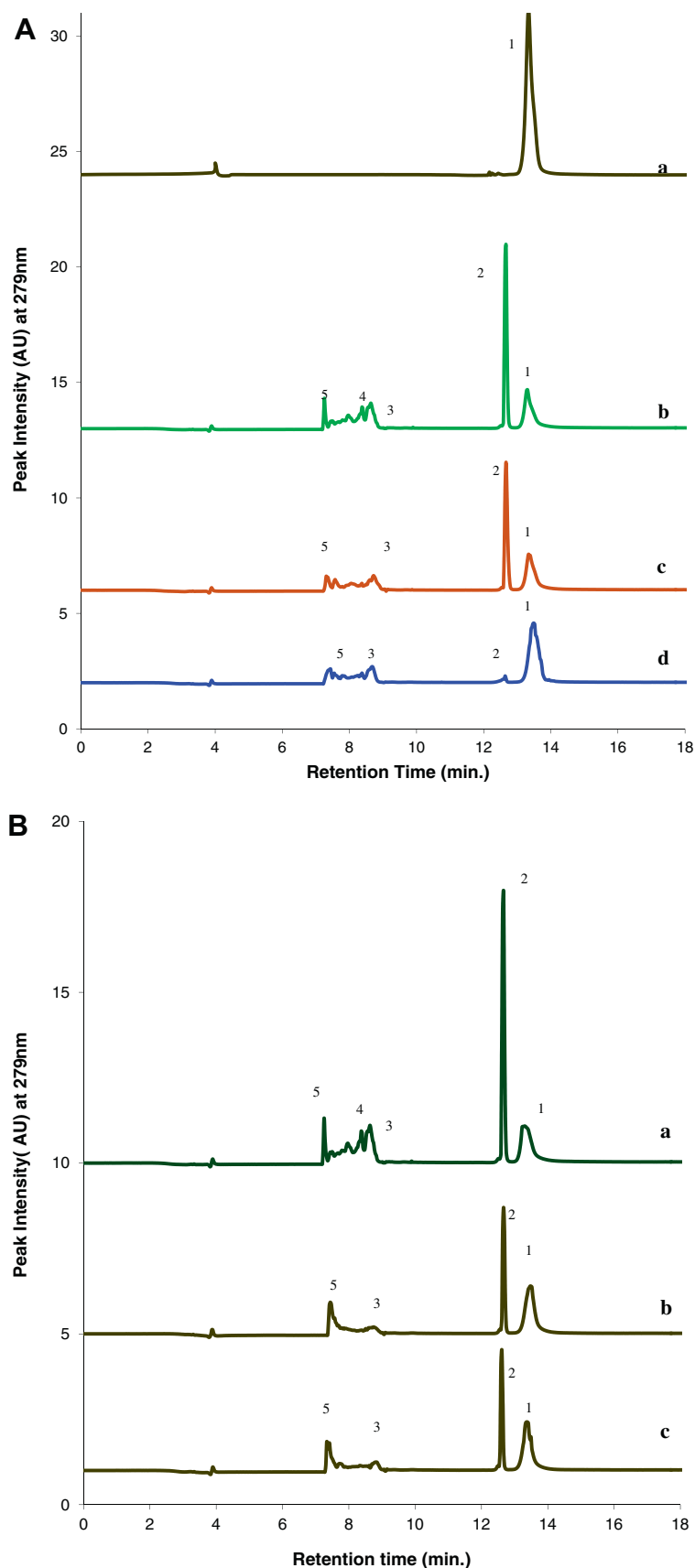
### 3.4. Changes of amino acid residues of HSA

Fig. 4A and B represents FTIR spectra of HSA–GA mixtures incubated for 10 days with and without 2GNP in the range of 1400–2000  $\text{cm}^{-1}$ . The secondary structure analysis was based on Amide-I and Amide-II bands, within the region 1300–2000  $\text{cm}^{-1}$  after subtraction of the background absorption. The spectra include two major bands: Amide I and Amide II transmittance bands, as depicted in Fig. 4A and B, appeared at a mean frequency of 1652  $\text{cm}^{-1}$  and at 1548  $\text{cm}^{-1}$  respectively, representing the amount of carbonyl and amino bonds in side chains of amino acid residues of HSA structure [18]. The corresponding spectra altered in shape as the HSA reaction with GA progressed, which indicated that the altered secondary structural elements were evolved throughout the time studied. These shifts in band positions of the spectra were attributable to alteration in HSA structure due to modification by GA and 2GNP.

The analysis of the structure of the Amide I and II bands in Fig. 4A and B indicated that there is 0.9% difference in transmittance between modified HSA by GA and native HSA.

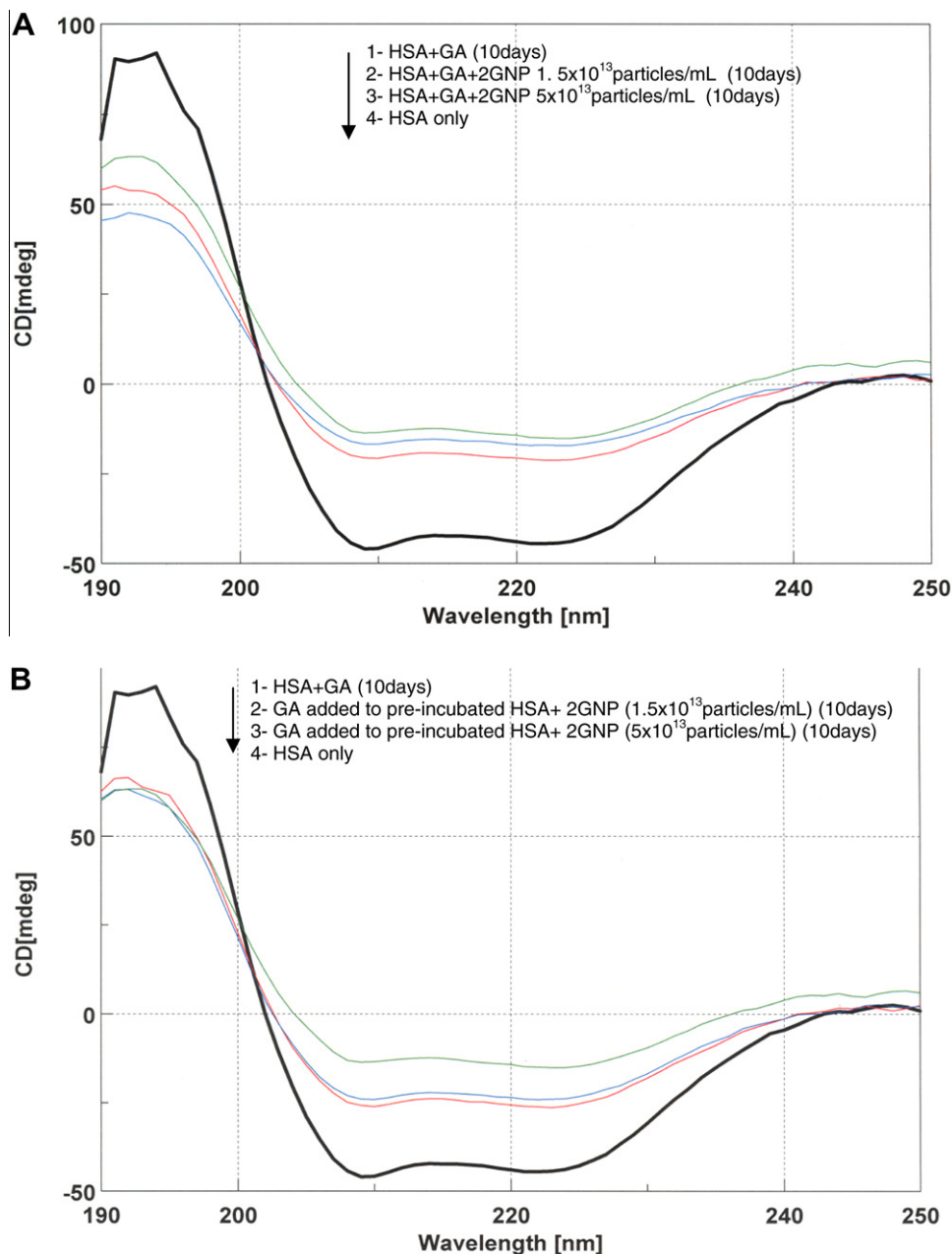
As shown in Fig. 4A, while the presence of 2GNP  $5 \times 10^{13}$  particles/mL and GA in HSA solution, transmittance of both amide bands I and II were minimally changed indicating more unaffected amide bonds and amino groups were present in the solution contained 2GNP  $5 \times 10^{13}$  particles/mL. Modified HSA in the presence of  $5 \times 10^{13}$  particles/mL 2GNP showed 0.6% transmittance difference whereas mixtures with  $1.5 \times 10^{13}$  particles/mL 2GNP showed no difference compared to control HSA–GA mixture without 2GNP. This indicates mixtures with  $5 \times 10^{13}$  particles/mL 2GNP, retained more unaffected carbonyl and amide bonds in HSA secondary structure compared to HSA–GA mixture, and HSA–GA with  $1.5 \times 10^{13}$  particles/mL 2GNP mixtures. This can be attributed to minimal secondary structural changes of the protein in the presence of  $5 \times 10^{13}$  particles/mL of 2GNP and this specifies more pronounced inhibition of HSA modification by  $5 \times 10^{13}$  particles/mL 2GNP.

Fig. 4B shows the FTIR spectrum of solutions that obtained from GA reacted with pre-incubated HSA–GNP mixtures. Compared to extensively glycated control HSA–GA, both FTIR spectra of 2GNP



**Fig. 2.** (A) Reversed phase HPLC elution profiles of HSA with GA mixtures after 10 days of incubation. (a) HSA, (b) HSA–GA mixtures without 2GNP, (c) HSA–GA with 2GNP ( $1.5 \times 10^{13}$  particles/mL), and (d) HSA–GA with 2GNP ( $5 \times 10^{13}$  particles/mL). (B) Reversed phase HPLC profiles of pre-incubated HSA with 2GNP. (a) HSA with GA incubated for 10 days, (b) GA added to pre-incubated HSA–2GNP ( $1.5 \times 10^{13}$  particles/mL) and further incubated for 10 days, and (c) GA added to pre-incubated HSA–2GNP ( $5 \times 10^{13}$  particles/mL) and further incubated for 10 days. All readings were taken in triplicates. UV absorbance was measured at 279 nm wavelength.





**Fig. 3.** CD profiles of (A) HSA–GA with and without 2GNP incubated for 10 days. (B) GA added to pre-incubated HSA–2GNP and further incubated. All samples were diluted  $2 \times 10^4$  times with deionized water before obtaining the CD profile. Repeat studies revealed no significant difference in CD profiles.

( $1.5 \times 10^{13}$  particles/mL or  $5 \times 10^{13}$  particles/mL) modified HSA with GA showed relatively small difference in transmittance after incubating 10 days. This shows that GA implicates similar structural changes to HSA when HSA was previously reacted with 2GNP. This observation is consistent of the HPLC and CD data of the current study, which provides evidence for concentration independent HSA structural changes induced by 2GNP.

#### 4. Discussion

The non-enzymatic glycation of proteins has been widely studied; this phenomenon has been found to play a major role in human physiology. The reactive carbonyl groups of sugars react with the nucleophilic amino groups of the amino acid residues of protein and form Schiff base adducts that can rearrange to form

AGE after a variety of chemical reactions [1]. Accumulation of AGEs, resulting from glycation, *in vivo* has been reported to account for many of the chronic complications of diabetes, including atherosclerosis, renal failure, cataract formation and Alzheimer's disease [3–5]. The current study made an effort to evaluate the influence of gold nano-particles on the AGE formation of HSA and GA, *in vitro*.

It is known that amino groups present on the amino acids side chains interact with gold colloids [6]. Although, methodological studies demonstrated that larger nanoparticles could aggregate, it has not been reported that 2GNP tends to aggregate while reacting with proteins. Nanoparticles have a very large surface-to-volume ratio, so that even a small amount of particles present extremely large surface areas available for protein binding.

It has been reported that the major serum proteins albumin, immunoglobulin and fibrinogen associate with a wide range of

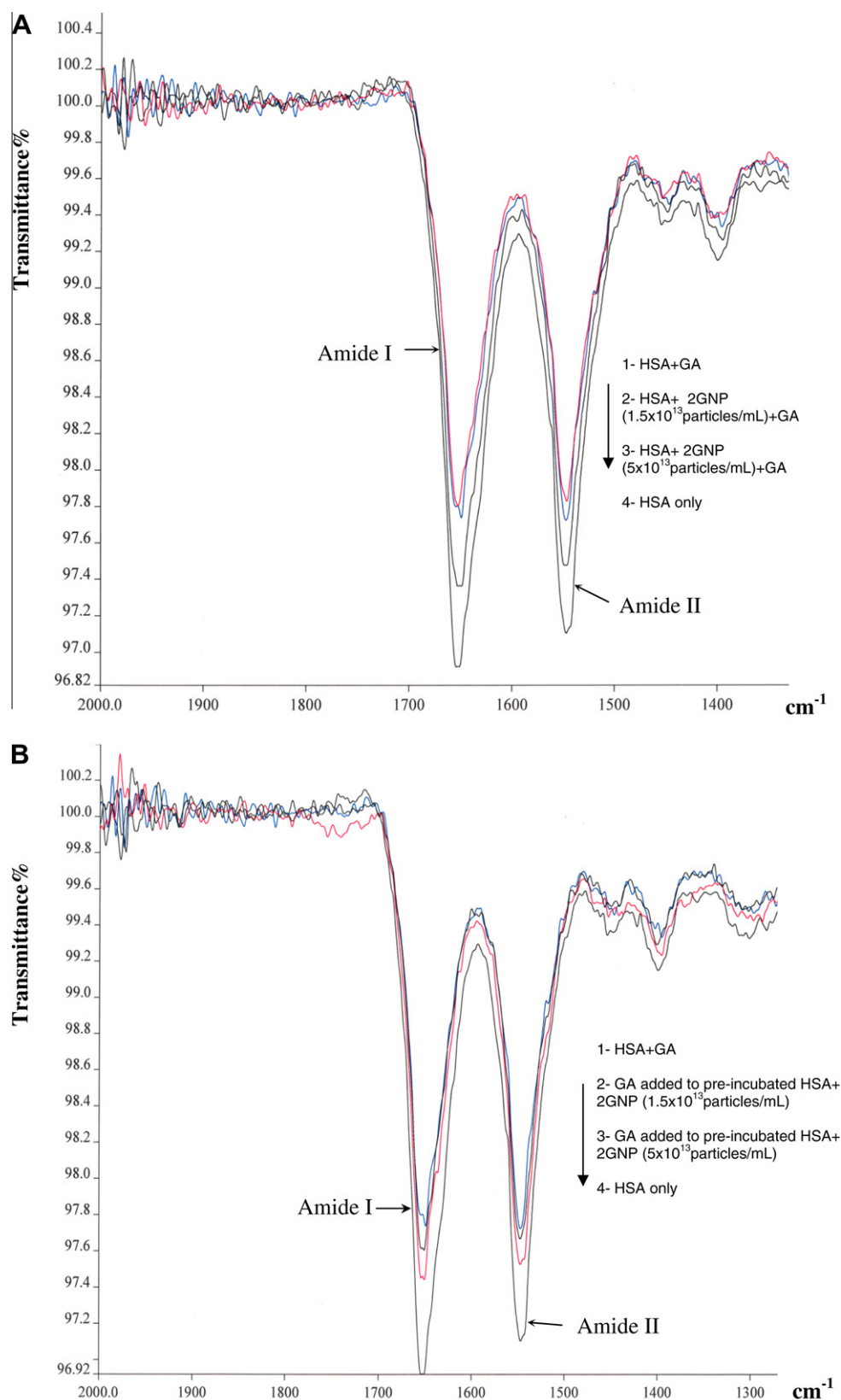


**Fig. 4.** FTIR profiles of Amide I and Amide II bands (A) HSA and GA mixtures with and without 2GNP. (B) GA added to pre-incubated HSA–GNP mixtures and further incubated. All FTIR data obtained after incubated for 10 days.

particles with a variety of sizes and seemingly produces different molecular compositions [19]. Due to its high abundance, albumin is widely experimented with larger sized nanoparticles (i.e.

20–50 nm) and these particles have a relatively low affinity to large proteins [18]. In contrast, this study indicates 2GNP, small nanoparticles, have a considerable influence in HSA–GA glycation reaction.

The incubation of HSA (35 mg/ml), GA (30 mM) in the presence of  $5 \times 10^{13}$  particles/mL of 2GNP resulted in a decrease in AGE formation of the protein and this finding was confirmed with a combination of analytical methods. Earlier studies in our lab reported that the GA readily reacts with a HSA [20] and CD spectra showed HSA was destabilized by GA. The present study reports that the reactivity of HSA and GA can be reduced by 2GNP and the destabilization of HSA by GA is also reduced in the presence of 2GNP in a concentration dependent manner. We hypothesize that 2GNP particles can react with free amino groups of certain common glycation sites of HSA and obstruct the amino groups from GA reactivity.

Some of the free amino groups of protein can react with gold nanoparticles by donating electrons to the 2GNP and 2GNP also can form electrostatic interactions with protonated amino groups.

The HPLC data confirms that the formation of AGEs was influenced by gold nanoparticles and demonstrated this interaction is a concentration-dependent process. Prior studies reported and anti-glycation activity of GNP on hemoglobin and crystalline protein [15]. Consistently, the present study confirms that HSA modification by GA in the presence of 2GNP shows evidence of reduction in non-enzymatic glycation, a situation that can cause changes in both the HSA structure and stability due to the reaction of HSA and 2GNP.

In summary, this study discloses that (i) gold nanoparticles of 2 nm in size can reduce the rate of non-enzymatic modification of HSA by GA and (ii) gold nanoparticles can change the secondary structure of HSA in a concentration independent manner.

In conclusion, the present study provides the insights of the potential applications of gold nanoparticles, which may help to reduce diabetic complications and chronic diseases related to non-enzymatic glycation. Findings of this study further support the view of the anti-glycation properties GNPs, and may offer useful link with therapeutic applications in reducing AGE related disease conditions.

## Acknowledgments

The project described was supported by funds from the NCRR/NIH Grant #PR016459 and the network institutions.

## References

- [1] L.C. Maillard, Action des acides aminés sur les sucres: formation des mélanoides par voie méthodique, C. R. Acad. Sci. 154 (1912) 66–68.

- [2] S.R. Thorpe, J.W. Baynes, Maillard reaction products in tissue proteins: new products and new perspectives, Amino Acids 25 (2003) 275–281.
- [3] E. Selvin, M. Steffes, H. Zhu, et al., Glycated hemoglobin diabetes and cardiovascular risk in non-diabetic adult, N. Engl. J. Med. 362 (2010) 800–810.
- [4] S.D. Yan, X. Chen, A.M. Schmidt, et al., Glycated tau-protein in Alzheimer's disease: a mechanism for induction of oxidant stress, Proc. Natl. Acad. Sci. USA 91 (1994) 7787–7791.
- [5] S. Horiuchi, Advanced glycation end products (AGE)-modified proteins and their potential relevance to atherosclerosis, Trends Cardiovasc. Med. 6 (1996) 163–168.
- [6] R. GhoshMoulick, J. Bhattacharya, C.K. Mitra, et al., Protein seeding of gold nanoparticles and mechanism of glycation sensing, Nanomedicine 3 (2007) 208–214.
- [7] Š. Miroslav, P. Zdeněk, Glycation of human serum albumin by D-glucose: a fluorescence quenching study, Collect. Czech. Chem. Commun. 62 (1997) 1815–1820.
- [8] V.L. Colvin, K.M. Kulinowski, Nano-particles as catalysts for protein fibrillation, Proc. Natl. Acad. Sci. USA 104 (2007) 8679–8680.
- [9] J. Klein, Probing the interactions of proteins and nanoparticles, Proc. Natl. Acad. Sci. USA 104 (2007) 2029–2030.
- [10] P. Mukherjee, R. Bhattacharya, N. Bone, et al., Potential therapeutic application of gold nanoparticles in B-chronic lymphocytic leukemia (BCLL) enhancing apoptosis, J. Nanobiotechnol. 5 (2007) 76–97.
- [11] Z. Krpetic, F. Porta, G. Scari, Selective entrance of gold nanoparticles into cancer cells, Gold Bull. 39 (2006) 65–68.
- [12] J.L. Burt, C. Gutiérrez-Wing, M. Miki-Yoshida, et al., Noble metal nanoparticles directly conjugated to globular proteins, Langmuir 20 (2004) 11778–11783.
- [13] M.E. Aubin, K. Hamad-Schifferli, Structure and function of nanoparticle-protein conjugates, Biomed. Mater. 3 (2008) 34–39.
- [14] S. Singha, J. Bhattacharya, H. Datta, et al., Anti-glycation activity of gold nanoparticles, Nanomedicine: NBM 5 (2009) 21–29.
- [15] J. Bhattacharya, S. Jasrapuria, T. Sarkar, et al., Gold nanoparticle based tool to study protein conformational variants: implications in hemoglobinopathy, Nanomedicine: NBM 3 (2007) 14–19.
- [16] R. GhoshMoulick, J. Bhattacharya, S. Roy, et al., Compensatory secondary structure alterations in protein glycation, Biochim. Biophys. Acta 1774 (2007) 233–242.
- [17] S. Sheikpranbabu, K. Kalishwaralal, K. Lee, et al., The inhibition of advanced glycation end-products-induced retinal vascular permeability by silver nanoparticles, Biomaterials 31 (2010) 2260–2271.
- [18] T. Cedervall, I. Lynch, S. Lindman, T. Berggard, Understanding the nanoparticle: protein corona using methods to quantify exchange rate and affinities of proteins for nanoparticles, Proc. Natl. Acad. Sci. USA 104 (2007) 2050–2055.
- [19] P. Aggarwal, J.B. Hall, C.B. McLeland, Nanoparticle interaction with plasma proteins as it related to particles biodistribution biocompatibility and to particle biodistribution therapeutic efficacy, Adv. Drug Delivery Rev. 61 (2009) 428–437.
- [20] U. Dutta, M.A. Cohenford, J.A. Dain, Monitoring the effect of glyceraldehyde glycation on the secondary structure human serum albumin and immunoglobulin G: an analysis based on circular dichroism thermal melting profiles and UV–fluorescence spectroscopy, Anal. Chim. Acta 558 (2006) 187–194.